



All-Sky Search for Transient Sources of Neutrinos Using Five Years of AMANDA-II Data

RODÍN PORRATA¹ FOR THE ICECUBE COLLABORATION

¹University of California at Berkeley, Department of Physics, Berkeley, CA 94270, USA

porrata@berkeley.edu

Abstract: Up to now, analyses of AMANDA data have been limited to searches for diffuse astrophysical sources, time-integrated searches for point sources, and searches for flares and bursts from preselected sources (AGN and GRB) over very limited timescales. However, multi-wavelength studies have shown that AGN and GRB emissions generally occur in exponential flares or bursts with strengths that can be much greater than that of the corresponding quiescent emission, and that the timescales for these violent outbursts can vary from milliseconds to months. Therefore, we are performing an all-sky search for transient sources of neutrinos with AMANDA data taken from the years 2000 to 2004 [1], surveying the largest range of timescales for which an improved signal to noise ratio can be obtained. In this report we describe a new analysis technique that utilizes an unbinned two-point correlation function which separates pairs of signal events from the atmospheric neutrino background by taking into account the probabilities for observing the given spatial separation, time separation, and total number of hit channels (NCH) of the events given both signal and background hypotheses. At the shortest timescales probed, this analysis achieves a differential fluence sensitivity, $\bar{\mathcal{F}}^0 = \left(\frac{E}{1\text{TeV}}\right)^\gamma \frac{d\bar{\mathcal{F}}}{dE}$, to flaring FR-I galaxies that is almost a factor of three better than the 5-year stacked point source sensitivity, assuming a spectral index, $\gamma = 2$, and a $\mathcal{F}_{\nu_\mu + \bar{\nu}_\mu} / \mathcal{F}_{\nu_e + \bar{\nu}_e}$ flavor ratio of one. If they produce events in the detector at all, fluences from such sources must be critically close to the detection threshold to avoid having been observed in other surveys, thus a pair search could provide the earliest detection of astrophysical neutrinos.

Introduction

Studying the space-time-energy properties of pairs of neutrinos has several advantages over other methods of searching for astrophysical sources.

1. We can search the whole sky for astrophysical sources in disregard of the scarcity of multi-wavelength information that could potentially aid such a search, allowing the possible detection of source classes that are dark at other wavelengths.
2. Since the search utilizes the energetic information that can be inferred from NCH data, it uses the same advantage that a diffuse search does to observe a faint astrophysical signal, however, unlike a diffuse analysis, correlated event searches are unaffected by a charm component.
3. If the number is sufficient, a pair search has the greatest sensitivity to detect very weak classes of astrophysical point sources, and is more powerful than searching for other multiplicities, e.g., pairs probe 84 % more space than triplets, while if present, a neu-

trino triplet will be counted as 3 pairs, with comparable significance.¹

The Time Variability of AGN and GRB

In summary, the activity of AGN and GRB [2][3][4][5][6][7][8], the primary astrophysical candidates associated with theorized hadronic processes inducing neutrino emission, suggests that we could observe astrophysical neutrinos arriving in bursts with almost any imaginable time difference. We assume that on a logarithmic scale, flare timescales are uniform.

1. Classes of point sources with N_e events per source and N_s objects will be expressed in this analysis as $N_p = N_s N_e (N_e - 1) / 2$ pairs, e.g., if a source like Mrk 421, for which there is 7 events observed in the integrated point source analysis, emits those neutrinos on a timescale less than one day, then it will appear in this analysis as 21 pairs – a situation that has a chance better than 50 % of producing a 5- σ discovery.

However, considering the differences in the astrophysical processes over different timescales, the pair search is separated into searches over several different timescales based upon the classes of objects that might be observed. Tab. 1 lists a possible way to construct the search categories. Optimization of the search strategy and calculation of the significance of the search results is conducted separately for each search timescale.

Flare Category	T_l / T_u	L
GRB / TeV SN / TeV AGN	1 s / 2 hr	A
GRB afterglow / TeV AGN	2 hr / 3 dy	B
Large scale AGN flare	3 / 30 dy	C
AGN high state period	30 / 100 dy	D

Table 1: Timescales over which we will search for various astrophysical categories: (1) category of objects, (2) minimum/maximum time between events (T_l/T_u), (3) label for this discussion.

Constraints and Background

The diffuse analysis [9] imposes the most stringent limit on the total number of neutrinos from all astrophysical sources integrated over the entire sky that could possibly be observed. For the 2000-2004 point source dataset, this translates to ~ 80 neutrinos assuming an E^{-2} source spectrum. We have used this number as the maximum number of neutrinos that we simulate for any of the source classes we consider.

While studying the response of the detector to background and potential astrophysical sources, the time-integrated point source analyses are able to average the detector efficiencies over time and right ascension (RA). However, this analysis probes the detector down to timescales of a second or less, so it can be strongly affected by the asymmetries of the detector. A new method of randomizing the data was developed that properly takes into account the asymmetries in the combined zenith (ZEN) and azimuth (AZ) distribution of events, the preferential occurrence of NCH values from certain AZ and ZEN directions, and the granularity of the detector on-periods. The ZEN and AZ of background events are sampled from the data itself and a smearing function is applied. The smearing function, determined by

MC, is the point spread function of the detector given an atmospheric neutrino spectrum. Times are sampled from a list of all possible detector on-periods for the entire 5 year analysis. Having obtained a map of the ZEN, AZ, and time of the events according to the efficiencies of the detector, the RA is calculated using the standard transformation. This method, comparable to *direct integration* [10], keeps all detector efficiencies intact, while producing a randomized sky-map of the data that is complete.

Search Technique

All pairs of neutrino events are compared. For each pair that falls within the minimum and maximum time differences given by the search class (see Tab. 1), ζ is calculated and if its value surpasses a predetermined threshold, ζ_c , the count of observed events is incremented. Once the tally is complete, the significance of the observation is determined using the Poisson p-value. To derive ζ , consider the likelihood ratio for the i th pair of events:

$$\mathcal{LR}_i = \frac{P(\text{NCH}_i|S) P(\log_{10}[\Delta t_i]|S) P(\psi_i|S)}{P(\text{NCH}_i|B) P(\log_{10}[\Delta t_i]|B) P(\psi_i|B)}$$

where:

$P(\text{NCH}_i|B)$ - The probability distribution for NCH, given a pair of background events. This is obtained by calculating the distribution of all combinations of NCH values from the data itself. Before this distribution is calculated, the values are standardized across 8 different declination bands by subtracting the median of the distribution and dividing by the inter-quartile difference, both declination dependent quantities. The standardization process removes to first order the geometric component of the variation of NCH values as a function of ZEN, leaving the spectral energy dependence intact.

$P(\log_{10}[\Delta t_i]|B)$ - The distribution of the logarithm of time differences of background pairs of events. This is obtained by fitting time differences of the data from 0.001 to 30 days with a power law. The result of the fit gives $P(\log_{10}[\Delta T]|B) \propto \Delta T^{0.98}$. This is in agreement with expectations that it should increase proportionally with the time difference. The fit is used to

obtain the probability of observing pairs of events that occur 0.01 days apart or less. For longer timescales the randomized time distribution is used directly.

$P(\psi_i|\mathbf{B})$ - The probability of observing a given spatial separation of background events is $\sim \rho_{bg} \sin \psi/2$, where ρ_{bg} is the local spatial density of background events. Since the background does not vary too quickly, and since an average over all directions is obtained when moving away from the point in question, this approximation is good enough.

$P(\text{NCH}_i|\mathbf{S})$ - The probability distribution for NCH given a pair of signal events. This is obtained from source MC, weighted according to an E^{-2} spectrum. This probability distribution is standardized using the same quantities used to standardize $P(\text{NCH}_i|\mathbf{B})$.

$P(\log_{10} \Delta t_i|\mathbf{S})$ - Based upon reviews of AGN and GRB activity, the central assumption of this work is that the distribution of flare/burst timescales is the scale invariant Jeffrey's prior [11], i.e., a *constant* for logarithmically sized bins.

$P(\psi_i|\mathbf{S})$ - The probability of observing a given separation in space of a pair of signal events from the same source. This is obtained from source MC data, weighted according to an E^{-2} spectrum. The PSF takes into account both the intrinsic $\nu_\mu \rightarrow \mu$ mismatch angle and the mismatch angle between the reconstructed muon and its true direction. Note that the PSF is evaluated at an angle, Ψ , which is half the separation angle, ψ , between the events.

According to the Neyman-Pearson Lemma, the quantity, $\zeta_i = \log_{10}(\mathcal{L}\mathcal{R}_i)$, represents one of the best possible ways of utilizing all the information we have discussed in order to provide evidence to decide whether the i th pair of events is an observation of signal or background. The choice of the value of ζ_c is optimized by maximizing the probability of producing a 5- σ detection. The analysis is run on 10,000 simulated experiments with pure background and 1000 simulated experiments that contain a small amount of simulated signal for different scenarios. The background and signal pairs are counted as a function of the cut on ζ and the significance of the observation is calculated for each experiment so that the detection probability can be estimated from the set of exper-

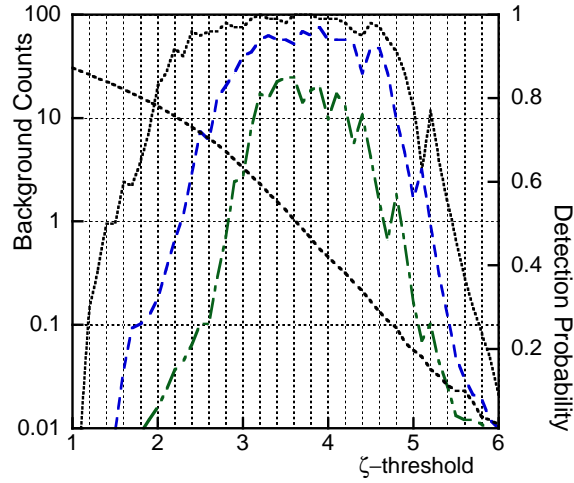


Figure 1: **Preliminary** probabilities for (from top to bottom) 3, 4, and 5- σ detections are plotted (units on r.h.s.) for a 2 hour search as a function of cut on ζ . The monotonically decreasing curve is the expected counts from background only. The time distribution of the signal is logarithmically uniform, 5.5 source pairs per $\log_{10}(\Delta T/\text{Days})$ extending from 10 seconds to 2 hours.

iments. For a search for GRB-timescale flares (A in Tab. 1), where the signal consists of ~ 16 sources distributed isotropically on the sky and distributed log-uniformly from 10 seconds to two hours, each source contributing two events to the dataset, the expected background is plotted in Fig. 1, as are the 3, 4, and 5- σ detection probabilities. Here it is seen that the 5- σ detection probability is maximal at $\zeta_c = 3.6$ where its value is better than 80%.

Results and Conclusions

The fluence sensitivity is given by

$$\bar{\mathcal{F}}_L^0 = \frac{\bar{\mu}_{90}}{n_s} \mathcal{F}_s^0$$

where \mathcal{F}_s^0 is the normalization constant on the differential fluence (the differential flux integrated over the duration of flaring events) of the signal model studied, n_s is the number of neutrino events that would be observed given such a fluence, and $\bar{\mu}_{90}$ is the Feldman-Cousins average upper limit given the background and no source

events [12]. For classes of objects with more than one member, n_s is the sum of contributions from each. Preliminary differential fluence sensitivities, as well as detection probabilities, are presented in Tab. 2 for two classes of objects that meet the requirements of the diffuse analysis. In Fig. 2 we plot the differential fluence

Cat.	N_s	$N_{\nu ps}$	$\varepsilon_{\mathcal{T}}$	\mathcal{F}_L^0	$P_{5-\sigma}$
A	20	2	0.78	2.70	99.6
B	27	3	0.44	8.2	86

Table 2: **Preliminary** differential fluence sensitivities and detection probabilities for representative source classes: (1) Category of objects, (2) no. of sources, (3) no. of neutrinos per source, (4) signal efficiency, (5) $\nu_\mu + \nu_\tau$ fluence sensitivity in units of $10^{-4} \text{ TeV}^{-1} \text{ cm}^{-2}$, (6) 5- σ detection probability (%), excluding our $N_T = 4$ trials factor.

sensitivities of GRB-timescale source classes for which the n th source has a relative strength given by [13] $\mu_n = \mu_0 n^{-\alpha} e^{-n/n_c}$. Our sensitivity to FR-I-like objects [14] (not including the brightest source, which is 3C-274, $\alpha = 0.65$) that produce Cat. A flares is $1.3 \times 10^{-3} \text{ TeV}^{-1} \text{ cm}^{-2}$ compared to the integrated stacking analysis [13] result of $3.4 \times 10^{-3} \text{ TeV}^{-1} \text{ cm}^{-2}$. Final results of

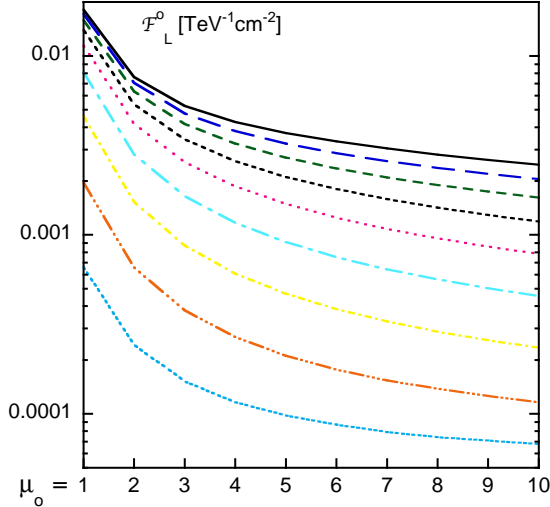


Figure 2: **Preliminary** fluence sensitivities for Cat. A objects characterized by α and μ_o . The curves, from top to bottom, are for $\alpha = 2$ to $\alpha = 0$ in steps of 0.25, assuming $n_c = 50$.

this survey will be presented in Tab. 3 at time of the conference. The results of this sensitivity study

Flare Category	ζ_c	μ_{bg}	n_{obs}	p-value
A	3.6	1.0	n_{obs}	p
B	2.14	20.9	n_{obs}	p
C	ζ_c	μ_{bg}	n_{obs}	p
D	ζ_c	μ_{bg}	n_{obs}	p

Table 3: **Preliminary** results of survey. (1) Category of objects, (2) optimized evidence threshold, (3) no. background pairs expected, (4) no. pairs observed, (5) significance, including N_T .

show the potential of this technique to search for weak astrophysical sources. This study will serve as the starting point for all-sky transient searches performed with the full IceCube detector.

References

- [1] A. Achterberg et al., Phys. Rev. D (accepted 2007).
- [2] J. A. Galdos et al., Nature, **38** 319 (1996).
- [3] D. Kniffen et al., ApJ **540** 184 (2000).
- [4] K. Hurley et al., Nature, **372** 652 (1994).
- [5] D. J. Thompson et al., ApJ. Supp. Ser., **157** 324 (2005).
- [6] P. L. Nolan, ApJ, **597** 615-627, (2003).
- [7] Valtaoja et al., ApJ Supp. Ser., **120** 95-99, (1999).
- [8] J. Albert et al., submitted to ApJ, (2007).
- [9] J. Hodges et al., Proc. 29th ICRC, Pune, India (2005).
- [10] R. Atkins et al., ApJ, **595**, 803-811 (2003).
- [11] P. Gregory, Cambridge Univ. Press 2005.
- [12] G. Feldman and R. Cousins, Phys. Rev. D, **57** 3873 (1998).
- [13] A. Achterberg et al., Astropart. Phys., **26** 282 (2006).
- [14] B. Fanaroff and J. Riley, MNRAS **167** (1974).